

Control of an Actuator DC Energy-saving Dedicated to the Electric Traction

Moez Hadj Kacem
Laboratory of Electronic and
Information Technology
(LETI-Sfax) Tunisia

Souhir Tounsi
Laboratory of Electronic and
Information Technology
(LETI-Sfax) Tunisia

Rafik Neji
Laboratory of Electronic and
Information Technology
(LETI-Sfax) Tunisia

ABSTRACT

The electric vehicle (V_e) is struck by their low autonomy. To remedy this problem, we opted for the choice of a converter structure in electromagnetic switch, since it has no power dissipation in switching and conduction.

The development of a control law of motorization continues saving energy and its implementation under the environment of MATLAB / SIMULINK, led to the scientific results of high level.

Keywords

electric vehicle, the DC motor (MCC), converter, design, analysis, finite element electromagnetic switch control.

Nomenclature

I	Current in permanent regim
Ecu	Thickness of the copper layer
Lsp	Average length of one turn
Ns	Number of winding spire
Sd	Main section of a tooth
Sc	Section of the wire
Ld	Width of the tooth
Bc	Maximal flux density in the ferro-magnetic core
Bd	Flux density in the left and right teeth
Bcs	Flux density in the yoke
μ_0	Air permeability
μ_r	Copper relative permeability
Hd	Height of the tooth
ρ	Copper resistivity
Ub	Amplitude of the switched voltage feeding the winding
Dco	Maximal opening of the ferro-magnetic core
xt	Displacement of the ferro-magnetic core
Hcu	Height of the winding
Ldc	Distance separating the winding and the right tooth
Eb	Length of the main tooth
V	Displacement speed of the ferro-magnetic core

Mt	Mass of the mobile core
Ke	electric constan
Ra	winding resistance
ia	Armature current
La	The inductance of the armature winding

1. INTRODUCTION

In light of high oil crises and atmospheric pollution in recent decades, vehicle electrification becomes a topical project. But the production of electric vehicles in large volumes is still hampered by their low autonomy and their relatively high cost.

Naturally, the MCC are driven at varying speed through a chopper IGBT leading to several problems [1] which include the floating potential, the tail current, the lath-up and static and dynamic problem [2] of losses. These problems lead to complications of the control circuit and to the requirement in most cases of the integration of a cooling system of the chopper. That's why we chose a structure of a converter to electromagnetic switches leading to the suppression of all these problems. The directive in an analytical model for sizing this type of switch is developed in conjunction with a validation study of complementarity and the finite element method.

The study of dynamic behavior of the engine showed that the switching frequency is low, which led us to integrate a low gear reduction ratio to reduce the frequency of magnetization of the engine, to solve the problem of compatibility of the type of switch in the overall system[3]. We also present a control strategy MCC saving energy. Indeed, when the VE operates in high acceleration regime (regime starts), the motor absorbs a strong current[4], since the forward drive of the carcass demand a high torque. To solve this problem leading to a high energy consumption, we chose to impose an increase of the excitation current proportional to an increase in dielectric constant at this operating regime. This control technology (Overfluxing) significantly reduces energy consumption. At high speeds, the electric constant is reduced to a value that ensures a maximum speed of 80km/h.

2. STRUCTURE OF THE STATIC CONVERTER

The structure of the chopper chosen for our application is illustrated by the following figure:

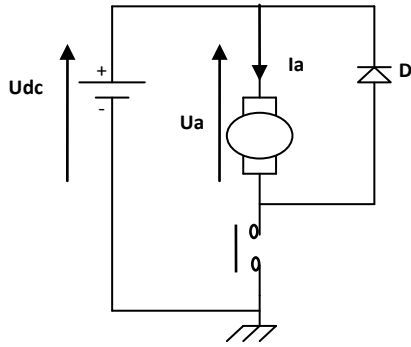


Fig 1: Structure diagram of the converter

The choice of this structure is justified by the fact. That a single switch that switches to the opening and closing and a single diode, which promotes the substantial absence of power dissipation [5]. Most of this structure has the advantage of relatively low cost compared to the structures of four-quadrant choppers.

2.1 Model

The converter model for electromagnetic switch is presented in the following figure [2]:

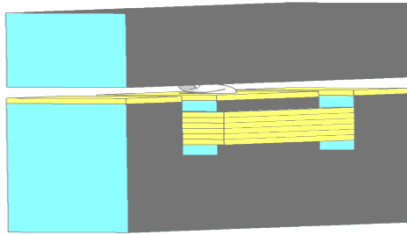


Fig 2: Converter model for electromagnetic switch

2.2 Principle of operation

This structure is composed by a mechanical contact normally closed S Fig3. The supply of the coil by a sufficient current causes attraction of the rod by induction phenomenon, and subsequently the change of state of the switch S. The de-excitation of the coil leads to the cancellation of the force of attraction of the rod, allowing the switch to return to its initial state.

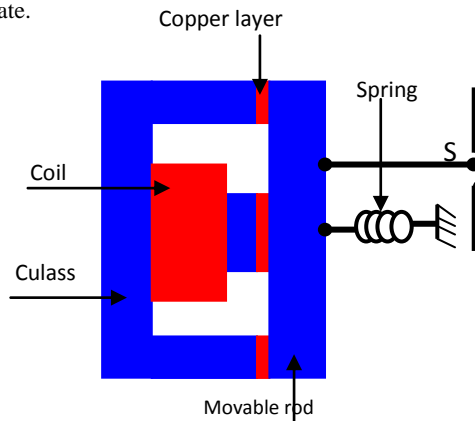


Fig 3: Arm of the static converter with electromagnetic switches

3. MODELING OF THE ELECTROMAGNETIC SWITCH

The design parameters of the winding generation are illustrated in figure 4 [2].

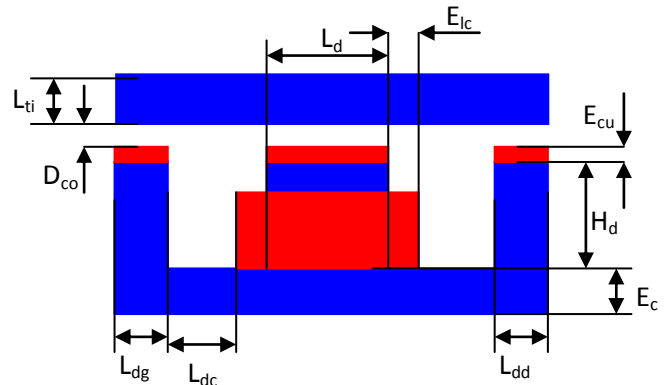


Fig 4: Design parameters

3.1 Electrical and geometrical parameters modeling

The flux density in the copper when the kernel is closed ferromagnetic, is deduced from the application of theorem amps:

$$B_{ec} = \mu_0 \times \mu_r \times \frac{N_s^2 \times I}{2 \times E_{cu}} \quad (1)$$

The thickness of the ferromagnetic core is derived from the application of the theorem of conservation of flow:

$$L_{ti} = \frac{B_{ec} \times L_d}{2 \times B_c} \quad (2)$$

The thickness of the cylinder head is expressed by the following relationship:

$$E_{cs} = \frac{B_{ec} \times L_d}{2 \times B_{cs}} \quad (3)$$

The winding resistance is expressed as follows:

$$R_{bob} = \frac{\rho \times N_s \times L_{sp}}{S_c} \quad (4)$$

The winding resistance of protection used to limit the winding current to the maximum current supported by the winding

The expression of the inductor winding.

$$L_b = \mu_0 \times N_s^2 \times \left(\frac{\frac{S_d}{2}}{2 \times (E_{cu} + D_{co} - x_t)} + \frac{H_{cu} \times E_b}{E_{ic} + L_{dc}} \right) \quad (5)$$

3.2 Modeling the force of attraction of ferromagnetic core

The attractive force of drift based on ferro-magnetic energy stored in the winding:

$$W_b = \frac{1}{2} \times L_b \times I^2 \quad (6)$$

This energy is transformed into mechanical energy of the core face ferromagnetic:

$$F \times V = \frac{1}{2} \times I^2 \times \frac{dL_b}{dx_t} \times \frac{dx_t}{dt} \quad (7)$$

Hence the force of attraction is deduced from the following relationship:

$$F = \frac{1}{2} \times I^2 \times \frac{dL_b}{dx_t} \quad (8)$$

3.3 Validation of finite element analysis model

The length of the coil of production is important, which reduces the three-dimensional effects, resulting in the maintaining of a two-dimensional model. Indeed, the model is made with measurements taken from the analytical calculation and is simulated for different static positions of the ferromagnetic core. The distribution of field lines is shown in Figure 5:

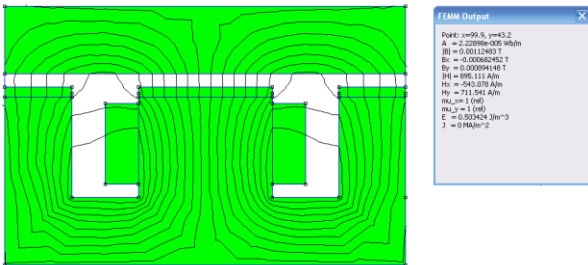


Fig 5: The distribution of the field lines

FIG 6 illustrates the evolution of the inductance value for different positions of the ferromagnetic core, calculated by the analytical method and finite element method:

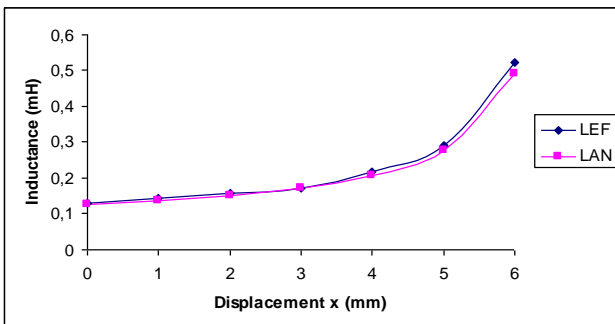


Fig 6: Inductance value for different positions of ferromagnetic core

This face shows that the two curves are combined, thus validating the analytical approach to modeling inductance. Figure 7 shows the evolution of the attraction force for different positions of the ferromagnetic core calculated by the analytical method and the finite element method:

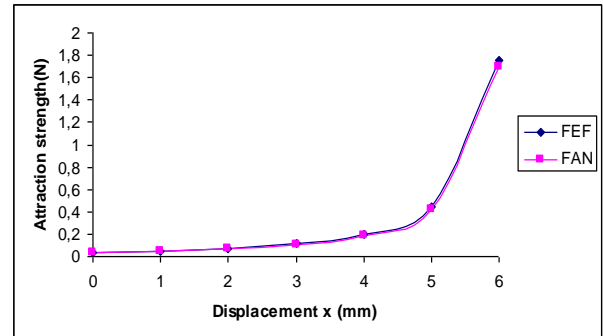


Fig 7: Evolution of the attraction for different positions of the ferromagnetic core

This face shows that the two curves are combined, thus validating the analytical modeling approach to the production of fully winding.

4. CONTROL OF THE DC MOTOR ENERGY SAVING TRACTION

4.1 Traction motor

The equation of electrical model of a DC motor is given by the following relationship:

$$U_a = R_a \times i_a + L_a \frac{di_a}{dt} + E_a(t) \quad (9)$$

The induced electromotive force of the motor is expressed by the following relationship:

$$E_a(t) = K_e \times \Omega \quad (10)$$

The electromagnetic torque developed by the motor is given by the following relationship:

$$C_{em} = K_e \times i_a \quad (11)$$

4.2 Model of converter

The signal for adjusting the supply voltage of the motor [6] so that the latter can develop the torque necessary to move the VE, is compared with a pointed triangular frequency much lower than the frequency of opening and closing of the electromagnetic switch. This comparison attack a living hysteresis between 0 and the DC bus voltage U_{dc} set for our application at 100 V in order to act on the pulse width of the control signals for adjusting the amplitude of current required to achieve a value of the electromagnetic torque sufficient to move the VE at the desired speed. The delay in opening the closure is modeled for the following transfer function:

$$Ft(s) = \frac{1}{1 + T_s \times S} \quad (12)$$

Where $T_s = T_{on} = T_{off} = 0.0047$ s : Time of delay in closing and opening.

The model of static converter implanted under the MATLAB Environment / SUMULINK is illustrated by the following figure: deduced from Ampere's theorem:

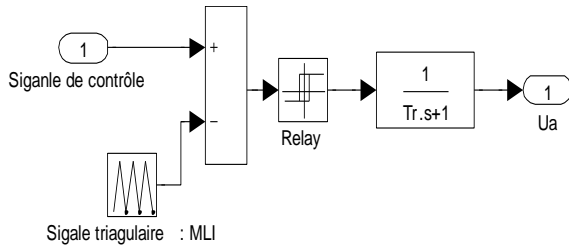


Fig 8: Model of converter

4.3 Equation of motion of the

The equation that governs the movement of VE is derived from the fundamental relation of dynamics [7, 8, 9]:

$$M_v \frac{dV}{dt} = r_d \times C_{em} - C_R(v) \quad (13)$$

Where M_v is the mass of VE, r_d is the reduction ratio of gear box and $C_R(V)$ is the resistive torque of the carcass:

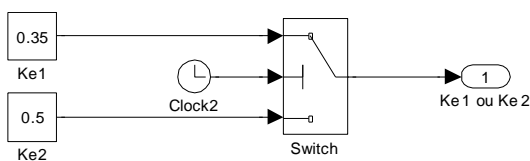
$$C_R(V) = R_r \times f_r \times M_v \times g + R_r \times \frac{M_{va} \times C_x \times S_f}{2} \times V^2 + R_r \times M_v \times g \times \sin(\lambda) \quad (14)$$

Where λ is the angle between the road with the horizontal and M_{va} is the density of air, C_x is the coefficient of air penetration, S_f is the front surface of the VE, f_r is the coefficient of resistance turnover and g is the acceleration due to gravity (with $g = 9.8$ Nm).

4.4 Equation of motion of the

Following a simulation at an average speed of EV, we set the start time or the electromagnetic torque and high (high current) to 685.

During the interval when the engine is running a scheme, we imposed a constant electric Ke larger than the constant for operation outside this regime [10].



Contrôleur de surfluxage

Fig 9: Controller Overfluxing.

Or 85 s is the startup time

$$Si t < 85 \text{ s } Ke = 0.85$$

$$Si t \geq 85 \text{ s } Ke = 0.35$$

And T_s is the delay time or the engine runs

4.5 Model of the global energy chain

The coupling of different models leads to the overall architecture of the power chain model implanted under the environment of MATLAB / SIMULINK following:

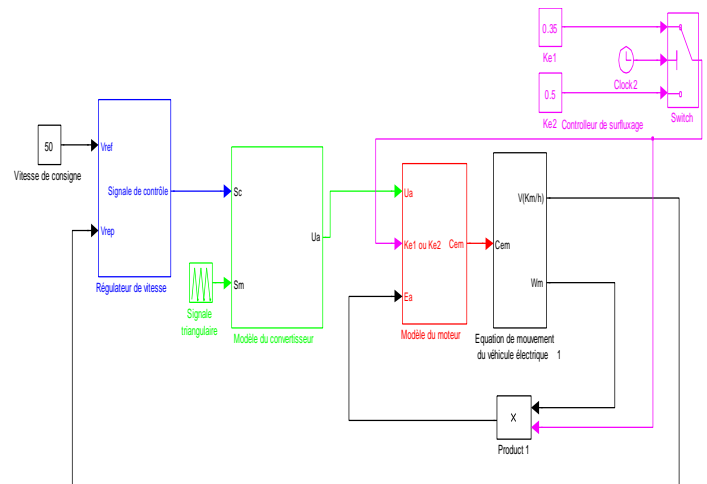


Fig 10: Model of the global chain of power EVs.

4.6 Descriptions of simulation results

Simulation results implanted under the environment of MATLAB / SIMULINK are:

4.6.1 And reference speeds of response:

From the characteristic speed of response to a power line model without integrated controller Overfluxing we set the starting time to 85 s, according to the figure below:

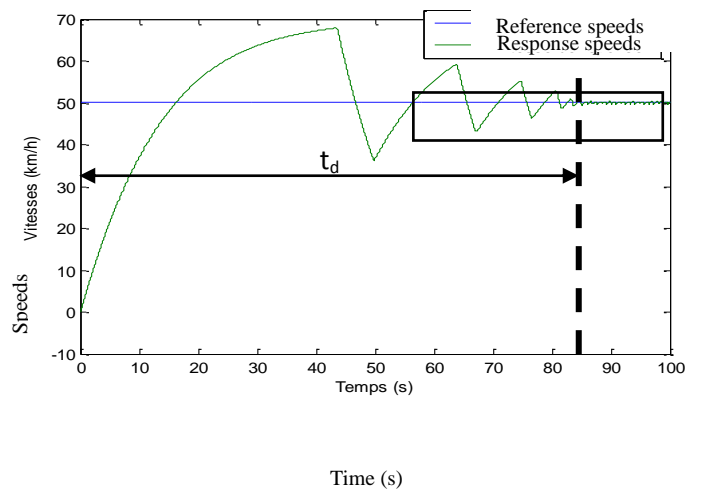


Fig 11: And reference speeds of response

4.6.2 Currents with and without overfluxing:

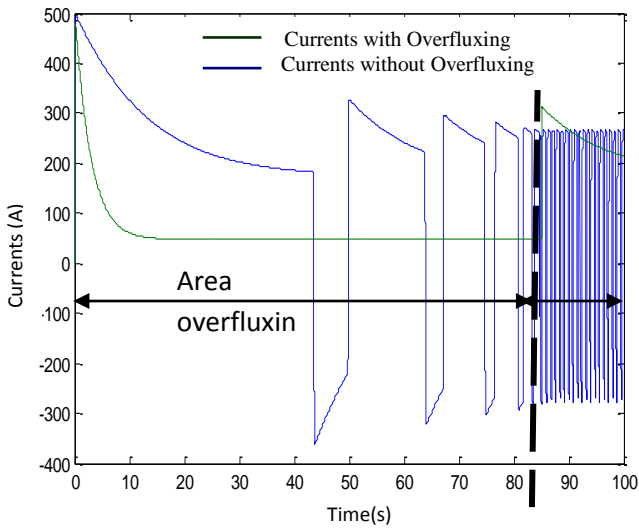


Fig 12: Currents with and without Overfluxing

This figure illustrates that the starting current undergoes a significant decrease with the controller Overfluxing, leading to reduced energy consumption of VEs.

4.6.3 Couples with and without Overfluxing:

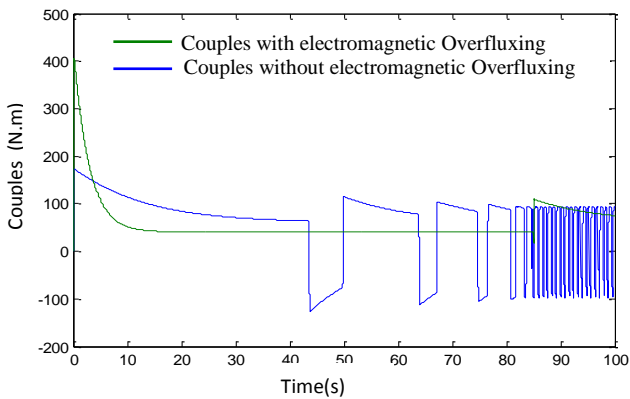


Fig 13: Couples with and without electromagnetic Overfluxing.

4.6.4 Powers with and without Overfluxing

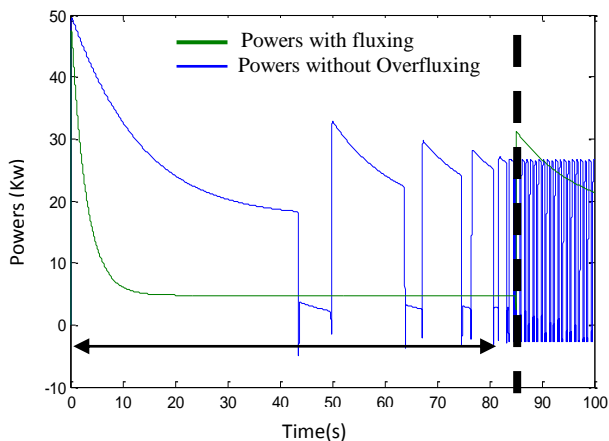


Fig 14: Powers with and without Overfluxing

This power is much lower for a chain with power controller Overfluxing.

4.6.5 Energy consumed with and without Overfluxing

The energy consumed is calculated from the relationship as follows:

$$W_{co} = \int P_{co} \times dt \quad (15)$$

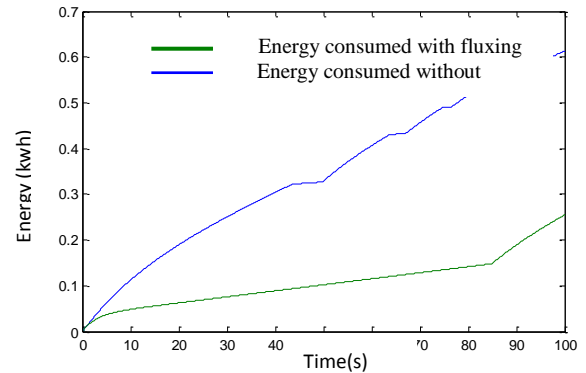


Fig 15: Energy consumption with and without Overfluxing.

The average value of this energy is without controller Overfluxing WCOM = 0.3444 Kw.h

It is much lower for a chain with power controller Overfluxing WCOM = 0.1080 Kw.h

4.6.6 Speed with and without Overfluxing

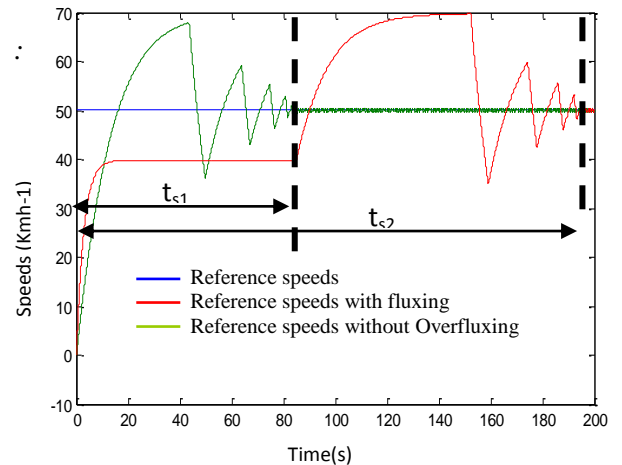


Fig 16: Speed with and without Overfluxing

Where ts1 is time to speed stability without Overfluxing and ts2 is the time to speed stability with Overfluxing: ts2 > ts1.

The drawback of the integration of a system Overfluxing Start is the importance of the stability time Overfluxing with speed relative to that without Overfluxing.

5. CONCLUSION

In this paper, we presented a systematic design methodology of a static converter with electromagnetic switches, dedicated to electric traction. This study succeeded in defining the parameters of manufacturing and control of the converter structure.

Our work has focused on the modeling and the development of a control law continues the engine chosen, reducing energy consumption and eventually leading to increased autonomy factor for the production of VEs in large series.

We presented a control strategy saving energy. This strategy is based on Overfluxing the DC motor during hard acceleration phase to reduce the current drawn by the motor. In this context, a chain model power, taking into account this technique, is implanted under the Environment MATLAB / SIMULINK.

Simulation results found are very encouraging. Perspective to this work as it will be very interesting in this integrated control laws and take into account the recovery of energy during phases of strong deceleration.

REFERENCES

- [1] A. AMMOUS, B. ALLARD, H. MOREL: "Transient Temperature Measurements and Modeling of the IGBT under short circuit". IEEE Transactions Electronics, vol. 13, No. 1, 1998,p.12-25.
- [2] S. TOUNSI, M.Hadj KACEM, R.NEJ: Design of Static Converter for Electric Traction" International Review of Electrical Engineering, IRE MOS Vol.3, N°6.
- [3] C. Houda ,B.Boumedyen,AM. Naceur, "Applikation of the forecasting parameters Horizon Moving in Diagnosis of broken bars in induction motor", 2012 International Conference on Computer Application and System Modeling. Vol 50 – N°17.
- [4] H. Yoshida, K. Kawata, Y. Fukuyama, S. Takayama, Y. Nakinishi: " A particle swarm optimization for reactive power and voltage control Considering safety assessment of tension", IEEE Transactions on Power Systems, 15 (2000) pp 1232-1239.
- [7] S. Tounsi, R. NEJI, F. SELLAMI: "Design of a radial engine for permanent magnet flux electric vehicle". EPE 2003 (10th European Conference on Power Electronics and Applications), 2-4 September in Toulouse-France, CD: PP151.
- [6] Blaabjerg, F., Consoli, A., Ferreira, Juge, et Wyk JD 2005 "The future of electronic power and conversion", IEEE Transaction on Power Electronics, vol. 20, p. 715-720. 20, pp. 715-720.
- [5] A .Mukhtiar, A. Larik Mohammad,R .Aslam Uqaili "Performance Analysis and Design Intelligent Power Controller Soft switched half-bridge DC / DC Converter using neural networks", 2012 International Conference on Computer Application and System Modeling. Vol 50 - No. 17.
- [8] R. NEJI, S. TOUNSI, F. SELLAMI: "Optimization and Design for a permanent magnet motor radial flow for electric vehicles". Journal of Electrical Systems (JES), 1-4 (2005 p. 47-68.Nvb2010.
- [9] K. Jouiliand and K. Ben Salem "Controlling a DC Motor for the Electric Traction". L.A memory in embedded system ISECS 2011.
- [10] S. TOUNSI, N. Ben Hadj, R. and F. SELLAMI NEJI: "Optimization of Design Parameters of the Eelectric Motor Maximize the range of Electric Vehicles". Review Internéational of Electrical Engineering (IREE), Vol 2, No 1 January-February 2007 ".